

# Resolving Hubble tension and locating missing baryons: Synergies between fast radio bursts and emerging cosmological probes

Peng-Ju Wu,<sup>1,\*</sup> Bo-Yang Zhang,<sup>2</sup> Ji-Guo Zhang,<sup>3</sup> Guo-Hong Du,<sup>3</sup> Shang-Jie Jin,<sup>3,4,5</sup> and Xin Zhang<sup>3,6,7,†</sup>

<sup>1</sup>*School of Physics, Ningxia University, Yinchuan 750021, China*

<sup>2</sup>*School of Physics and Electronic Information Engineering,*

*Ningxia Normal University, Guyuan 756000, China*

<sup>3</sup>*Liaoning Key Laboratory of Cosmology and Astrophysics,*

*College of Sciences, Northeastern University, Shenyang 110819, China*

<sup>4</sup>*Department of Physics, University of Western Australia, Perth WA 6009, Australia*

<sup>5</sup>*Research Center for the Early Universe, Graduate School of Science,*

*The University of Tokyo, Tokyo 113-0033, Japan*

<sup>6</sup>*Key Laboratory of Data Analytics and Optimization for Smart Industry (Ministry of Education),*

*Northeastern University, Shenyang 110819, China*

<sup>7</sup>*National Frontiers Science Center for Industrial Intelligence and Systems Optimization,*

*Northeastern University, Shenyang 110819, China*

Two of the most pressing challenges in cosmology are the persistent discrepancy in measurements of the Hubble constant, referred to as the Hubble tension, and the deficit of baryons in the local Universe, known as the missing baryon problem. Fast radio bursts (FRBs) encode the integrated electron column density along their lines of sight, offering a unique probe of both the cosmic expansion rate ( $H_0$ ) and the baryon density ( $\Omega_b$ ). However, constraints from FRBs alone suffer from a severe  $H_0$ – $\Omega_b$  degeneracy that prevents them from resolving either problem independently. We show that this degeneracy can be broken by combining FRBs with other emerging probes whose degeneracy directions differ in the  $H_0$ – $\Omega_b$  plane. Specifically, we quantify three multi-messenger approaches: FRBs paired with gravitational wave (GW) standard sirens, strong gravitational lensing (SGL) time delays, and 21 cm intensity mapping (IM). The combinations FRB+GW, FRB+SGL, and FRB+21 cm IM each deliver simultaneous constraints on  $H_0$  and  $\Omega_b$  better than (1%, 1%) in the  $\Lambda$ CDM model, (1.5%, 2%) in the  $w$ CDM model, and (2%, 3.5%) in the CPL model. Moreover, in a model-independent framework, both FRB+GW and FRB+SGL constrain  $H_0$  and  $\Omega_b$  to better than (1%, 2%) precision. These results demonstrate that the synergy between FRBs and other emerging probes holds great promise for resolving the Hubble tension and locating the missing baryons.

## I. INTRODUCTION

A profound crisis in modern cosmology arises from a set of persistent observational tensions that challenge the robustness of the standard  $\Lambda$  cold dark matter ( $\Lambda$ CDM) paradigm. Among these, two discrepancies have garnered particular attention for both their statistical significance and their implications for fundamental physics: the Hubble tension and the missing baryon problem [1–5]. The Hubble tension reflects the  $> 5\sigma$  discrepancy between the Hubble constant value measured from the cosmic microwave background (CMB) data by the Planck satellite  $H_0 = 67.4 \pm 0.5 \text{ km/s/Mpc}$  [6], and the higher value derived from distance-ladder measurements by the SH0ES collaboration  $H_0 = 73.04 \pm 1.04 \text{ km/s/Mpc}$  [2]. The missing baryon problem highlights the apparent shortfall in the observed inventory of baryonic matter at low redshifts relative to the cosmic baryon density predicted by the CMB analyses ( $\Omega_b \sim 0.05$ ) [6]. In both cases, the tension lies between early- and late-Universe determinations based on distinct methodologies and assumptions. Resolving them requires precise, independent measurements

from alternative probes to discern whether the discrepancies originate in new physics, unmodeled astrophysics, or hidden systematics.

Fast radio bursts (FRBs)—millisecond-duration radio transients that appear randomly across the sky—emerge as a promising new probe for this purpose [7–30]. As an FRB propagates through the ionized intergalactic medium (IGM), its signal interacts with free electrons, resulting in a frequency-dependent time delay quantified by the dispersion measure (DM). Observed DMs of FRBs significantly exceed the contribution expected from the Milky Way, indicating their extragalactic origins [31–33], with the exception of one Galactic burst [34, 35]. Since IGM constitutes the dominant baryonic reservoir along the line of sight, the IGM component of DM accumulates with redshift and thus can be considered as an indicator of the distance to the FRB source. This quantity is proportional to the product  $H_0\Omega_b$ , so that FRB observations alone can constrain only this degenerate combination, precluding independent determination of either parameter. To unlock the full potential of FRBs in resolving cosmological tensions, this degeneracy must be broken. This can be achieved by combining FRBs with complementary probes that either provide an independent measurement of  $H_0$  or exhibit a distinct degeneracy direction in the  $H_0$ – $\Omega_b$  plane.

In this paper, we assess the potential of future FRB

\* [wupengju@nxu.edu.cn](mailto:wupengju@nxu.edu.cn)

† Corresponding author; [zhangxin@neu.edu.cn](mailto:zhangxin@neu.edu.cn)

observations in combination with three emerging cosmological probes—gravitational wave (GW) standard sirens, strong gravitational lensing (SGL) time delays, and neutral hydrogen 21 cm intensity mapping (IM)—to provide simultaneous and precise measurements of  $H_0$  and  $\Omega_b$ . GW standard sirens provide a direct measurement of the luminosity distance  $D_L$  [36, 37], which scales as  $D_L \propto 1/H_0$ . This offers a distance estimate independent of the electromagnetic cosmic distance ladder, although it depends on accurate modeling of gravitational waveforms for calibration. SGL time delays, on the other hand, yield the so-called time-delay distance  $D_{\Delta t}$ , a geometric quantity constructed from angular diameter distances to the lens, to the source, and between them [38]. Since all angular diameter distances scale linearly with  $1/H_0$ , this composite distance inherits the same  $1/H_0$  dependence. In contrast, 21 cm IM measures the baryon acoustic oscillation (BAO) feature in the large-scale structure, providing simultaneous constraints on both the angular diameter distance  $D_A$  and the Hubble parameter  $H$  at the effective redshift of the survey [39]. While  $D_L \propto 1/H_0$  and  $H(z) \propto H_0$ , the physical interpretation of these observables depends critically on the absolute scale of the BAO ruler, i.e., the sound horizon at radiation drag  $r_d$ . This scale is determined by early-Universe physics and is itself a sensitive function of both  $H_0$  and  $\Omega_b$  [40]. Consequently, measurements of  $D_A/r_d$  and  $H(z)r_d$  do not directly yield  $H_0$  and  $\Omega_b$  in isolation, but instead produce constraints that are strongly degenerate between these two parameters. By combining FRBs with these complementary probes, the individual parameter degeneracies can be broken, enabling simultaneous constraints on  $H_0$  and  $\Omega_b$ .

Our primary objective is to assess how effectively the proposed synergistic approaches can break the characteristic degeneracy between  $H_0$  and  $\Omega_b$ , thereby deriving novel constraints on these two fundamental parameters. This paper is structured as follows. In Section II, we describe the simulation of future observational data for the four emerging probes based on specific experimental configurations. In Section III, we present the constraint results and make relevant discussions. Finally, we summarize our conclusions in Section IV.

## II. DATA SIMULATION

In this section, we generate mock observations for four emerging probes using representative next-generation facilities. For simulations, we adopt the flat  $\Lambda$ CDM model with Planck 2018 parameters:  $H_0 = 67.26 \text{ km/s/Mpc}$ ,  $\Omega_m = 0.317$ ,  $\Omega_b = 0.0495$ , and  $\Omega_K = 0$  [6].

### A. SKA-era FRB observations

The DM contribution from IGM relates to cosmology, and its average value is calculated by

$$\overline{\text{DM}}_{\text{IGM}}(z) = \frac{3cH_0\Omega_b}{8\pi Gm_p} \int_0^z \frac{(1+z')f_{\text{IGM}}(z')f_e(z')dz'}{E(z')}, \quad (1)$$

where  $c$  is the speed of light,  $G$  is Newton constant,  $m_p$  is the proton mass,  $f_e(z) = Y_H \chi_{e,H} + Y_{He} \chi_{e,He}/2$ , with  $Y_H = 3/4$  and  $Y_{He} = 1/4$  being the mass fractions of hydrogen and helium, and  $\chi_{e,H} = 1$  and  $\chi_{e,He} = 1$  being the ionization fractions, respectively.  $f_{\text{IGM}} \simeq 0.83$  is the baryon mass fraction in the IGM [5]. The uncertainty of  $\text{DM}_{\text{IGM}}$  can be written as

$$\sigma_{\text{DM}_{\text{IGM}}} = \left[ \sigma_{\text{obs}}^2 + \sigma_{\text{MW}}^2 + \sigma_{\text{IGM}}^2 + \left( \frac{\sigma_{\text{host}}}{1+z} \right)^2 \right]^{1/2}. \quad (2)$$

Here, we adopt  $\sigma_{\text{obs}} = 0.5 \text{ pc cm}^{-3}$  from published data [33, 41],  $\sigma_{\text{MW}} = 10 \text{ pc cm}^{-3}$  for the Milky Way contribution,  $\sigma_{\text{IGM}} \simeq 0.2 \text{ DM}_{\text{IGM}} z^{-1/2}$  accounting for the baryon inhomogeneity in IGM [42], and  $\sigma_{\text{host}} = 60 \text{ pc cm}^{-3}$  for the host galaxy contribution [10, 26].

In order to mock detectable FRBs, we need to choose a redshift distribution for FRBs. The common assumption is that FRBs' population tracks the star formation history (SFH). However, the CHIME/FRB catalog has ruled this out. In this paper, we adopt the power-law model of redshift distribution to simulate the FRB data, and the event rate of FRB is

$$N_{\text{SFH}}(z) = (1+z)^\gamma \mathcal{N}_{\text{SFH}} \frac{\dot{\rho}_*(z) D_C^2(z)}{H(z)(1+z)} e^{-D_L^2(z)/[2D_L^2(z_{\text{cut}})]}, \quad (3)$$

where  $(1+z)^\gamma$  refers to the delay with respect to SFH with  $\gamma = -1.1$ ,  $\mathcal{N}_{\text{SFH}}$  is a normalization factor,  $D_C$  is the comoving distance, and  $z_{\text{cut}} = 1$  is a cutoff, which reflects the decline in detected FRBs beyond it due to the instrumental signal-to-noise threshold. The density evolution form of SFH is parameterized as [43, 44]

$$\dot{\rho}_*(z) = \frac{(1+z)^{2.6}}{1 + ((1+z)/3.2)^{6.2}}. \quad (4)$$

For cosmological constraints, we need to estimate the FRB event rate. According to the estimation of the FRB detection event rate by the upcoming Square Kilometer Array (SKA) in Ref. [16], the 10-year observation of the SKA would detect  $\mathcal{O}(10^5 - 10^6)$  FRBs. Assuming that 10% of the detected FRBs can be well localized to confirm their host galaxies, there are still  $\mathcal{O}(10^4 - 10^5)$  FRBs with redshifts available for parameter inference. In this work, we consider a normally expected scenario of  $N_{\text{FRB}} = 100,000$  for the 10-year operation of SKA.

## B. ET-era GW observations

GWs can serve as standard sirens, since the GW waveform carries the information of the luminosity distance to the source. We simulate the GW standard sirens based on the third-generation GW detector, Einstein Telescope (ET), and assume that the GWs are from the binary neutron star (BNS) mergers. For the redshift distribution of BNSs, we adopt the form [45]

$$P(z) \propto \frac{4\pi D_C^2(z)R(z)}{H(z)(1+z)}, \quad (5)$$

where  $D_C$  is the comoving distance and  $R(z)$  is the time evolution of the burst rate with the form [46, 47]

$$R(z) = \begin{cases} 1+2z, & z \leq 1, \\ \frac{3}{4}(5-z), & 1 < z < 5, \\ 0, & z \geq 5. \end{cases} \quad (6)$$

We calculate the central value of luminosity distance in the flat  $\Lambda$ CDM model. The total errors of  $D_L$  consist of the instrumental error, weak lensing error, and peculiar velocity error,

$$\sigma_{D_L} = \sqrt{(\sigma_{D_L}^{\text{inst}})^2 + (\sigma_{D_L}^{\text{lens}})^2 + (\sigma_{D_L}^{\text{pv}})^2}. \quad (7)$$

For the  $\sigma_{D_L}^{\text{inst}}$  calculation, we refer the readers to Refs. [45, 48–54]. The errors caused by the weak lensing and peculiar velocity of the GW source can be found in Refs. [55, 56]. The  $D_L$ -redshift relation can be established, once the electromagnetic counterpart of the GW source is detected by optical telescopes. ET is expected to detect 1000 GW events from BNSs within  $z \lesssim 5$ , as the expectation of its 10-year operation [45, 57]. We simulate a sample of 1000 GW standard sirens.

## C. LSST-era SGL observations

SGL is a rare astronomical phenomenon where photons from a distant source are deflected by the gravity of intervening mass overdensities (e.g., galaxies, groups, clusters) as they propagate to Earth's detectors. SGL time delays provide a geometric probe of the universe. When the background source exhibits intrinsic flux variability, monitoring the lensed images allows a measurement of the arrival time differences between multiple images [38]. For a pair of images  $i$  and  $j$ , this time delay is given by

$$\Delta t_{ij} = \frac{D_{\Delta t}}{c} \left[ \frac{(\vec{\theta}_i - \vec{\beta})^2}{2} - \psi(\vec{\theta}_i) - \frac{(\vec{\theta}_j - \vec{\beta})^2}{2} + \psi(\vec{\theta}_j) \right], \quad (8)$$

where  $\vec{\beta}$  and  $\vec{\theta}_i$  are the angular positions of the source and the image  $i$ , respectively, and  $\psi$  is the lensing potential. The cosmological information is encapsulated in the

time-delay distance, defined as

$$D_{\Delta t} \equiv (1 + z_l) \frac{D_l D_s}{D_{ls}}. \quad (9)$$

where  $z_l$  is the lens redshift,  $D_l$ ,  $D_s$  and  $D_{ls}$  are the angular diameter distances to the lens, to the source, and between the lens and source, respectively. A measurement of the time delay, combined with models for the lens potential and the source position, yields a constraint on the distance ratio  $D_l D_s / D_{ls}$ . Since this ratio scales inversely with the Hubble constant, time-delay observations provide a direct avenue to constrain  $H_0$ . We simulate a sample of 55 time-delay events based on the Large Synoptic Survey Telescope (LSST). We generate the event redshifts using the code from Ref. [58] and calculate the time-delay distances within the fiducial model, assuming a 5% relative uncertainty for each measurement [59].

## D. HIRAX-era 21 cm IM observations

The 21 cm IM technique enables the measurement of the BAO signal by mapping the collective 21 cm emission from the neutral hydrogen (H1) in galaxies. We mock 21 cm IM observations based on the Hydrogen Intensity and Real-time Analysis eXperiment (HIRAX) [60]. The modeling begins with the mean 21 cm brightness temperature, given by

$$\bar{T}_b(z) = 188 h \Omega_{\text{HI}}(z) \frac{(1+z)^2}{E(z)} \text{ mK}, \quad (10)$$

where  $\Omega_{\text{HI}}(z)$  is the neutral hydrogen density fraction. Considering the effect of redshift space distortions, the signal covariance can be written as [39]

$$C^S = \frac{\bar{T}_b(z_i) \alpha_{\perp}^2 \alpha_{\parallel}}{D_C^2 D_{\nu}} (b_{\text{H1}} + f \mu^2)^2 \exp(-k^2 \mu^2 \sigma_{\text{NL}}^2) \times P(k), \quad (11)$$

where  $k$  is the wave vector,  $\mu$  is the cosine between  $\vec{k}$  and the line of sight direction,  $D_{\nu}(z) = c(1+z)^2 / H(z)$ , and the scaling factors are defined as  $\alpha_{\perp} \equiv D_A^{\text{fid}}(z) / D_A(z)$  and  $\alpha_{\parallel} \equiv H(z) / H^{\text{fid}}(z)$ . Here,  $b_{\text{H1}}$  is the H1 bias,  $f(z)$  is the linear growth rate,  $\sigma_{\text{NL}}$  parametrizes the non-linear dispersion scale, and  $P(k)$  is the matter power spectrum, which can be generated by CAMB [61]. The total covariance is modeled as the sum of three components:

$$C^T = C^S + C^N + C^F, \quad (12)$$

where the instrumental noise  $C^N$  is derived from HIRAX specifications, including system temperature  $T_{\text{sys}}$ , a survey area of 15,000 deg<sup>2</sup>, an observation time of 10,000 hours, and dish characteristics. The residual foreground term  $C^F$  is modeled under the assumption that foreground removal reduces contamination to a negligible level; further details can be found in Ref. [39].

Measurement uncertainties on the cosmological observables are forecast using the Fisher matrix formalism. We

focus on the parameter set  $\mathbf{p} = \{D_A(z), H(z), f\sigma_8(z)\}$  within independent redshift bins of width  $\Delta z = 0.1$  over  $0.8 < z < 2.5$ . For each redshift bin, the Fisher matrix is computed as:

$$F_{ij} = \frac{1}{8\pi^2} V_{\text{bin}} \int_{-1}^1 d\mu \int_{k_{\text{min}}}^{k_{\text{max}}} k^2 dk \frac{\partial \ln C^T}{\partial p_i} \frac{\partial \ln C^T}{\partial p_j}, \quad (13)$$

where  $V_{\text{bin}}$  is the comoving survey volume of the bin. The resulting Fisher matrices serve as inverse covariances for  $\{D_A, H, f\sigma_8\}$ . The central values of the observables are computed within the flat  $\Lambda$ CDM framework. Note that for cosmological parameter inference, we restore the sound horizon scale. That is, we employ the dimensionless observables  $\{D_A/r_d, c/(H \times r_d), f\sigma_8\}$  to constrain cosmological parameters. Here, the comoving sound horizon at the baryon drag epoch is calculated as

$$r_d = \int_{z_d}^{\infty} \frac{c_s(z)}{H(z)} dz, \quad (14)$$

where the sound speed is  $c_s(z) = c/\sqrt{3[1 + R_b a(z)]}$  with  $R_b = 3\Omega_b/(4\Omega_\gamma)$ , and the drag redshift  $z_d$  is computed as [40]:

$$\begin{aligned} z_d &= 1048 [1 + 0.00124(\Omega_b h^2)^{-0.738}] [1 + g_1(\Omega_m h^2)^{g_2}], \\ g_1 &= \frac{0.0783}{(\Omega_b h^2)^{0.238} [1 + 39.5(\Omega_b h^2)^{0.763}]}, \\ g_2 &= \frac{0.56}{1 + 21.1(\Omega_b h^2)^{1.81}}. \end{aligned} \quad (15)$$

In Fig. 1, we present the simulated observational data from FRBs, GW standard sirens, SGL time delays, and 21 cm IM surveys, based on specific experiments. In generating the mock data, we fix the fiducial (central) values and do not include their statistical fluctuations. This is justified for three reasons: (i) forecast analyses focus on parameter uncertainties rather than central values; (ii) fixing a common fiducial cosmology avoids artificial tensions when combining the four probes; and (iii) it ensures that the contours clearly illustrate how parameter degeneracies are broken through probe synergy.

### III. RESULTS AND DISCUSSIONS

In this section, we report the constraint results from four emerging probes and their synergies. We consider three cosmological models: (i) the  $\Lambda$ CDM model with a constant dark energy equation of state (EoS)  $w(z) = -1$ ; (ii) the  $w$ CDM model—the simplest dynamical dark energy model with a constant but free EoS  $w(z) = w$ ; and (iii) the CPL model—a parameterized dynamical dark energy model with a time-varying EoS given by  $w(z) = w_0 + w_a z/(1+z)$  [62, 63]. We adopt the Markov chain Monte Carlo method to infer the probability distributions of cosmological parameters by maximizing the likelihood  $\mathcal{L} \propto \exp(-\chi^2/2)$ , with  $\chi^2$  being the chi-squared statistic,

which quantifies the discrepancy between the theoretical predictions and the observational data. We measure the convergence of chains by checking that all parameters have  $R - 1 < 0.01$ , where  $R$  is the potential scale reduction factor of the Gelman-Rubin diagnostics. The  $1\sigma$  (68.3% confidence level) and  $2\sigma$  (95.4% confidence level) posterior distribution contours for  $H_0$  and  $\Omega_b$  are shown in Fig. 2, and the  $1\sigma$  errors for the marginalized parameter constraints are summarized in table. I.

TABLE I. Cosmological constraints on the  $\Lambda$ CDM,  $w$ CDM, CPL, and cosmography models from multi-messenger probes: FRB, GW, SGL, 21 cm IM, and their combinations. Here,  $H_0$  is in units of km/s/Mpc. The notation “N/A” indicates cases where the data provide insufficient constraining power to yield a meaningful limit on the parameter.

Probe	$\sigma(H_0)$	$\sigma(\Omega_b)$	$\sigma(\Omega_m)$	$\sigma(w/w_0)$	$\sigma(w_a)$
<b><math>\Lambda</math>CDM model</b>					
FRB only	N/A	0.034	0.0038	—	—
GW only	0.54	N/A	0.014	—	—
SGL only	0.75	N/A	N/A	—	—
21 cm IM only	N/A	0.011	0.0042	—	—
FRB+GW	0.24	0.00027	0.0037	—	—
FRB+SGL	0.44	0.00035	0.0037	—	—
FRB+21 cm IM	0.46	0.00030	0.0028	—	—
<b><math>w</math>CDM model</b>					
FRB only	N/A	0.034	0.0044	0.052	—
GW only	1.2	N/A	0.020	0.15	—
SGL only	2.1	N/A	0.21	1.2	—
21 cm IM only	N/A	0.012	0.0043	0.029	—
FRB+GW	0.51	0.00075	0.0042	0.047	—
FRB+SGL	0.65	0.00083	0.0043	0.050	—
FRB+21 cm IM	0.79	0.00075	0.0027	0.023	—
<b>CPL model</b>					
FRB only	N/A	0.035	0.054	0.14	0.84
GW only	1.9	N/A	0.059	0.28	1.7
SGL only	2.8	N/A	0.13	0.85	N/A
21 cm IM only	N/A	0.014	0.026	0.20	0.61
FRB+GW	0.99	0.0015	0.052	0.12	0.74
FRB+SGL	1.2	0.0017	0.055	0.13	0.78
FRB+21 cm IM	0.93	0.0012	0.011	0.083	0.29
<b>Cosmography (model-independent)</b>					
	$\sigma(H_0)$	$\sigma(\Omega_b)$	$\sigma(q_0)$	$\sigma(j_0)$	$\sigma(s_0)$
FRB only	N/A	0.034	0.078	0.27	0.26
GW only	1.2	N/A	0.13	0.44	0.25
SGL only	2.0	N/A	0.33	0.57	1.2
FRB+GW	0.61	0.00090	0.059	0.20	0.20
FRB+SGL	0.66	0.00094	0.067	0.22	0.22

In the  $\Lambda$ CDM framework, combining FRBs with complementary probes yields dramatic improvements in constraining both  $H_0$  and  $\Omega_b$ , successfully breaking the inherent degeneracy in the dispersion measures. The FRB+GW synergy delivers the most powerful constraints, achieving  $\sigma(H_0) = 0.24$  km/s/Mpc and  $\sigma(\Omega_b) = 0.00027$ , corresponding to precisions of 0.36% and 0.55%, respectively. The  $H_0$  constraint tightens by 56% compared to the GW-only measurement  $\sigma(H_0) = 0.54$  km/s/Mpc. FRB+SGL provides  $\sigma(H_0) = 0.44$  km/s/Mpc and  $\sigma(\Omega_b) = 0.00035$ , corre-

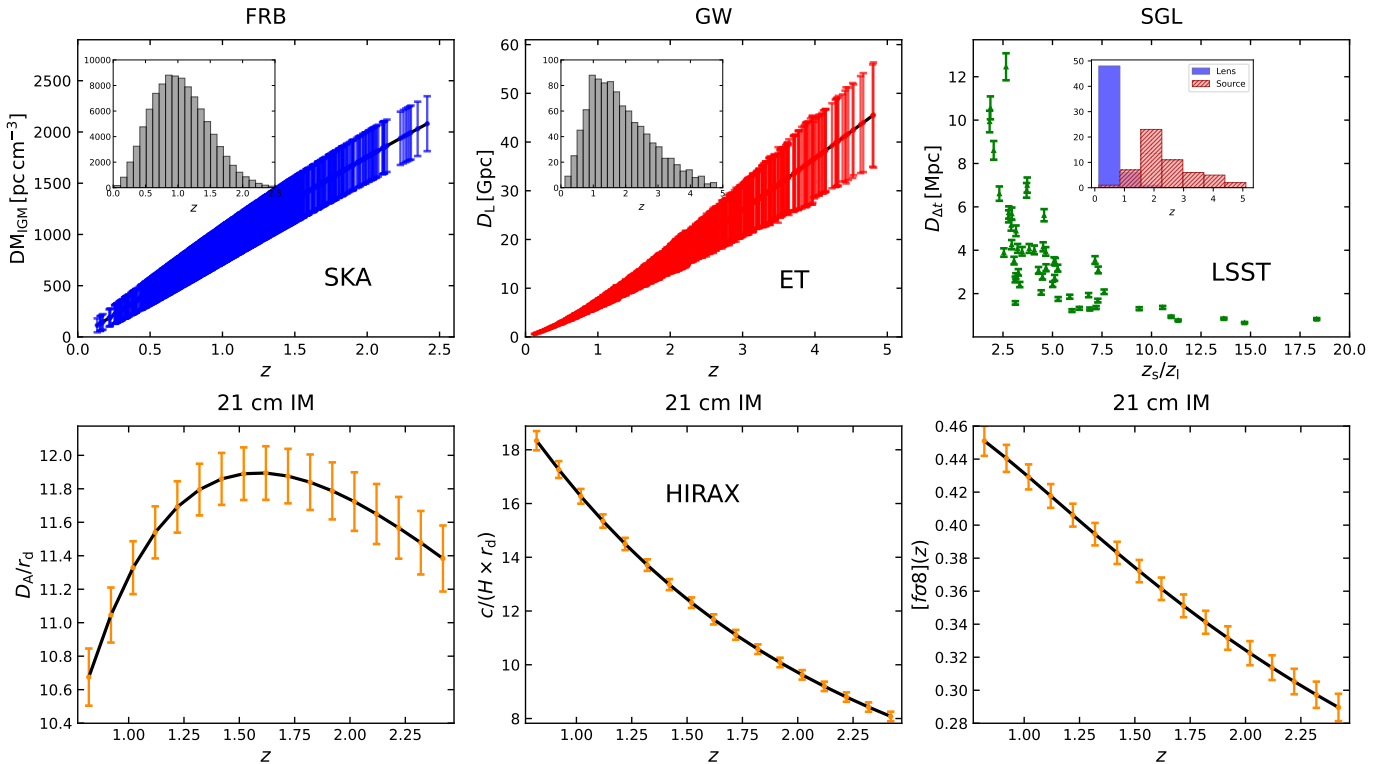


FIG. 1. Simulated observational data for four emerging cosmological probes: FRBs from SKA (top left); GW standard sirens from ET (top middle); SGL time delays from LSST (top right); and 21 cm IM from HIRAX (bottom three panels). For the FRB, GW, and SGL data, we show not only the measurement uncertainties but also the redshift distributions of the simulated samples.

sponding to relative errors of 0.65% and 0.71%, respectively. The  $H_0$  constraint tightens by 41% compared to the SGL-only result  $\sigma(H_0) = 0.75$  km/s/Mpc. Meanwhile, the FRB+21 cm IM combination yields  $\sigma(H_0) = 0.46$  km/s/Mpc and  $\sigma(\Omega_b) = 0.00030$  (0.68% and 0.61% relative errors). All three combinations can constrain the parameters  $H_0$  and  $\Omega_b$  to better than 1% precision.

In the  $w$ CDM model, introducing dark energy equation of state variability degrades constraints as the additional parameter covaries with cosmic expansion history. The FRB+GW combination still provides the strongest constraints, achieving  $\sigma(H_0) = 0.51$  km/s/Mpc and  $\sigma(\Omega_b) = 0.00075$ , corresponding to precisions of 0.76% and 1.5%, respectively. The  $H_0$  constraint tightens by 58% compared to the GW-only measurement  $\sigma(H_0) = 1.2$  km/s/Mpc. The FRB+SGL synergy yields  $\sigma(H_0) = 0.65$  km/s/Mpc and  $\sigma(\Omega_b) = 0.00083$  (0.97% and 1.7% relative errors), with the  $H_0$  constraint improving by 69% over the SGL-only measurement  $\sigma(H_0) = 2.1$  km/s/Mpc. In addition, FRB+21 cm IM produces  $\sigma(H_0) = 0.79$  km/s/Mpc and  $\sigma(\Omega_b) = 0.00075$  (1.2% and 1.5% relative errors). All three combinations maintain precision better than 1.5% for  $H_0$  and better than 2% for  $\Omega_b$ , even in this extended model.

In the CPL parameterization, allowing time-varying dark energy EoS through  $w_0$  and  $w_a$  further expands

parameter degeneracies, yet FRB synergy maintains remarkable constraining power. FRB+GW delivers  $\sigma(H_0) = 0.99$  km/s/Mpc and  $\sigma(\Omega_b) = 0.0015$ , corresponding to precisions of 1.5% and 3.0%, respectively. The  $H_0$  constraint tightens by 48% compared to the GW-only result  $\sigma(H_0) = 1.9$  km/s/Mpc. FRB+SGL provides  $\sigma(H_0) = 1.2$  km/s/Mpc and  $\sigma(\Omega_b) = 0.0017$  (1.8% and 3.4% relative errors), with the  $H_0$  constraint improving by 57% over the SGL-only measurement  $\sigma(H_0) = 2.8$  km/s/Mpc. We find that the FRB+21cmIM combination yields the best performance in this model. Specifically, FRB+21 cm IM achieves  $\sigma(H_0) = 0.93$  km/s/Mpc and  $\sigma(\Omega_b) = 0.0012$  (1.4% and 2.4% relative errors). Despite the expanded parameter space, all parameter combinations continue to constrain  $H_0$  within 2% and  $\Omega_b$  within 3.5%, demonstrating the robustness of our methodology.

The constraining power on parameters beyond  $H_0$  and  $\Omega_b$  varies significantly across different synergies. In the  $\Lambda$ CDM model, FRB+GW or FRB+SGL improve the constraint on  $\Omega_m$  by only 2.6% compared to FRB alone. In contrast, FRB+21 cm IM provides a gain of approximately 26%. In the  $w$ CDM model, FRB+GW or FRB+SGL yields only marginal improvements on  $\Omega_m$  and  $w$ , with precision gains of less than 10% compared to the FRB-only constraints. In stark contrast, FRB+21 cm IM dramatically enhances the precision, re-

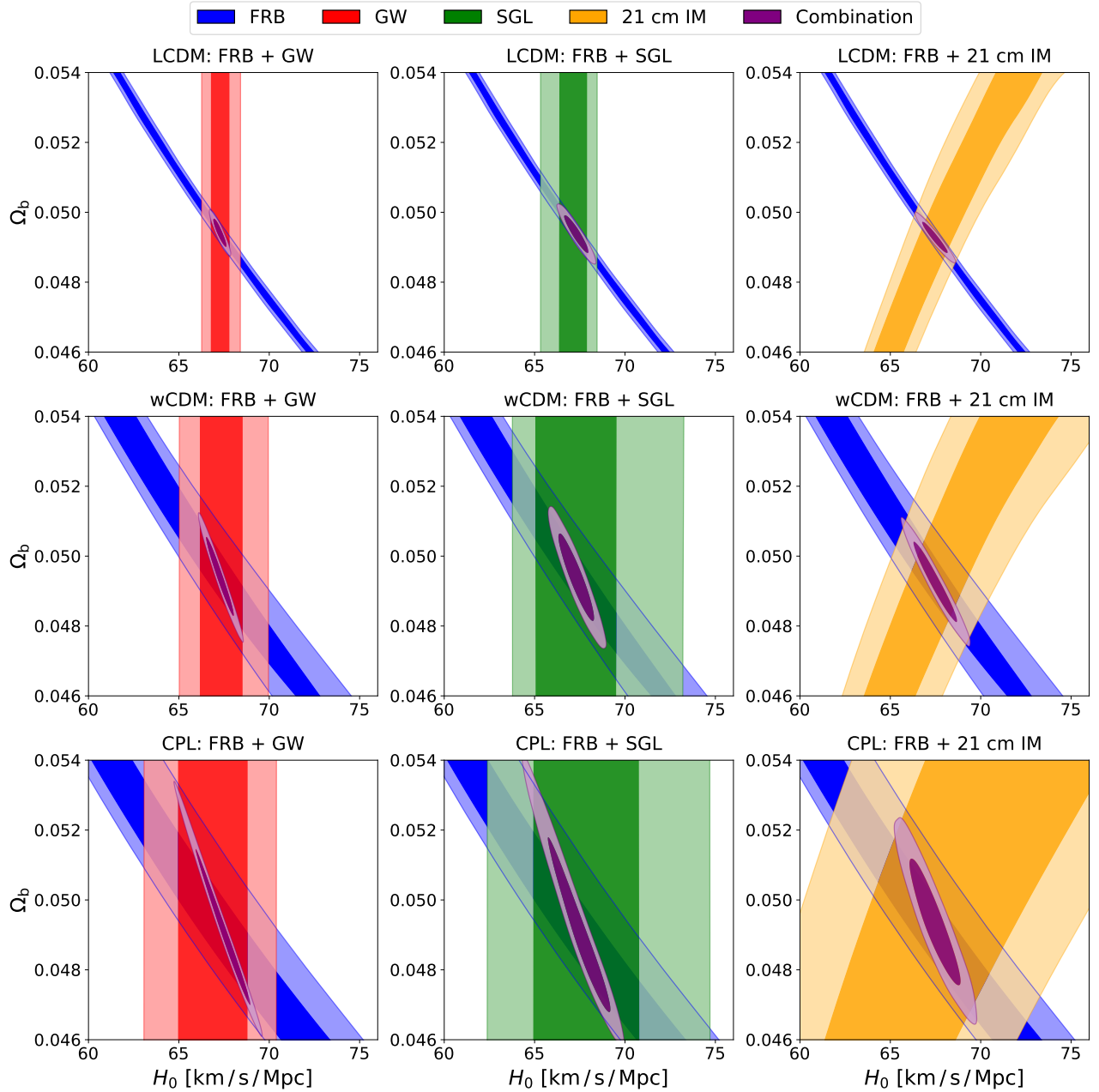


FIG. 2. Two-dimensional posterior distribution contours in the  $H_0 - \Omega_m$  plane for the  $\Lambda$ CDM,  $w$ CDM, and CPL models: constraints from the simulated FRB, GW, SGL, 21 cm IM, FRB+GW, FRB+SGL, and FRB+21cmIM data.

ducing the uncertainties on  $\Omega_m$  and  $w$  by approximately 39% and 56%, respectively. This trend is amplified in the CPL model. Here, the constraints on  $\Omega_m$ ,  $w_0$ , and  $w_a$  see only  $< 12\%$  improvements from FRB+GW or FRB+SGL, whereas FRB+21 cm IM provides a transformative gain of nearly 80%, 41%, and 65%, respectively. Therefore, for efforts aimed at concurrently enhancing the constraints on  $H_0$  and  $\Omega_b$  while achieving substantial gains on other cosmological parameters, FRB+21 cm IM emerges as the most compelling observational strategy.

All the models discussed above depend on particular

dark energy property assumptions. It is therefore essential to pursue model-independent outcomes, which necessitates further investigation. The cosmographic analysis avoids parametric dark energy assumptions entirely, instead expanding the distance-redshift relation in terms of Hubble constant, deceleration  $q_0$ , jerk  $j_0$ , and snap  $s_0$  parameters. In a homogeneous and isotropic universe described by the FLRW metric, the 3th order Taylor expansion for Hubble parameter around  $z = 0$  can be written

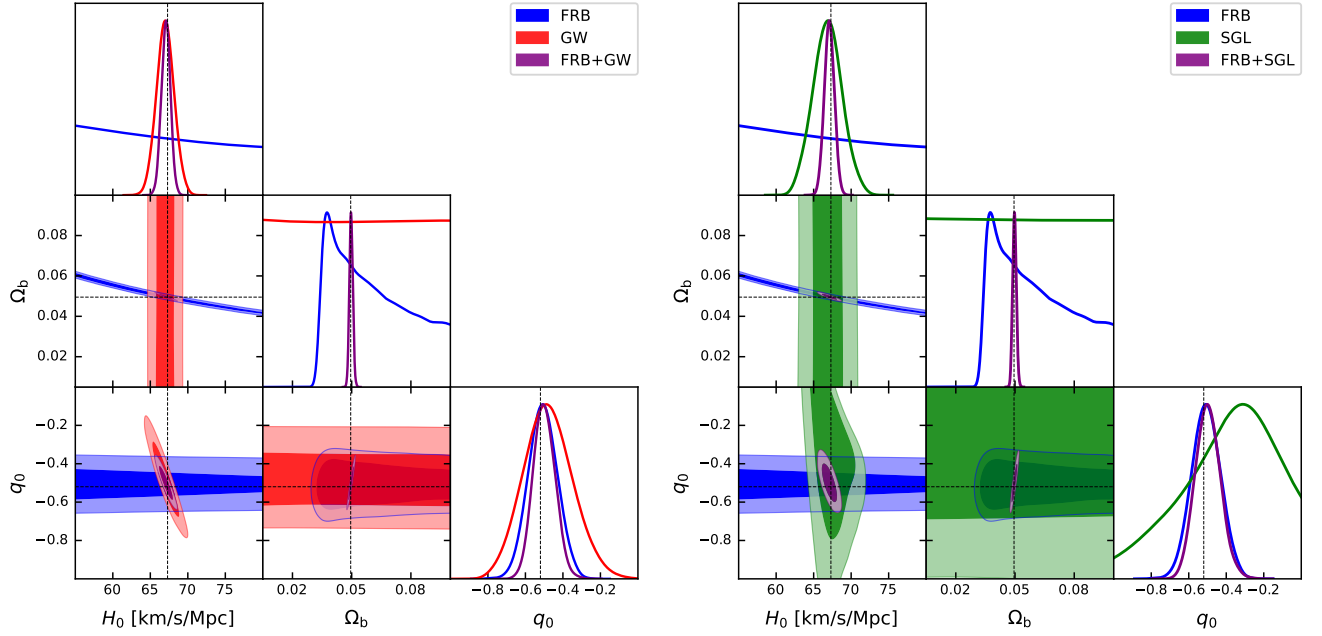


FIG. 3. Constraints on cosmographic parameters derived from FRB, GW, and FRB+GW in the left panel, and from FRB, SGL, and the joint FRB+SGL probe in the right panel.

as

$$H(z) \simeq H_0 + H_{10}z + H_{20} \frac{z^2}{2!} + H_{30} \frac{z^3}{3!} + \mathcal{O}(z^4), \quad (16)$$

where  $H_{i0}$  refers to the  $n$ -th derivative of Hubble parameter at present time, specifically

$$\begin{aligned} H_{10} &= H_0(q_0 + 1), \\ H_{20} &= H_0(j_0 - q_0^2), \\ H_{30} &= H_0(-4j_0q_0 - 3j_0 + 3q_0^3 + 3q_0^2 - s_0). \end{aligned} \quad (17)$$

The cosmographic parameters are defined as the scale factor derivatives with respect to cosmic time:

$$q \equiv -\frac{1}{aH^2} \frac{d^2a}{dt^2}, j \equiv \frac{1}{aH^3} \frac{d^3a}{dt^3}, s \equiv \frac{1}{aH^4} \frac{d^4a}{dt^4}. \quad (18)$$

In the model-independent framework, FRB+GW achieves  $\sigma(H_0) = 0.61$  km/s/Mpc (0.91%) and  $\sigma(\Omega_b) = 0.00090$  (1.8%), while FRB+SGL yields  $\sigma(H_0) = 0.66$  km/s/Mpc (0.98%) and  $\sigma(\Omega_b) = 0.00094$  (1.9%). Importantly, as presented in Fig. 3, the derived parameters are basically unbiased for the parameters  $H_0$  and  $\Omega_b$ , i.e., the fiducial values of parameters fall into the central part of  $1\sigma$  confidence regions, so the methods are convincing. The constraints on  $H_0$  and  $\Omega_b$  are comparable to those obtained in the  $w$ CDM model: both FRB+GW and FRB+SGL constrain  $H_0$  and  $\Omega_b$  to better than (1%, 2%) precision. In cosmography, the FRB+21 cm IM synergy cannot be used, because the expansion cannot be performed accurately up to the early universe (e.g., the last scattering). In this scenario, we can only treat the

sound horizon as a free parameter. However, in that case, 21 cm IM cannot provide meaningful constraints on  $H_0$  and  $\Omega_b$ , and there is no degeneracy between these two parameters. Consequently, combining 21 cm IM with FRBs does not significantly improve the constraints on these parameters. If we introduce a prior on the sound horizon from the early universe, we can constrain  $H_0$  and break the degeneracy between  $H_0$  and  $\Omega_b$  in FRBs. However, this approach contradicts our original goal of resolving the Hubble tension without relying the early-universe observations. To achieve this goal, any connection with CMB or BBN observations should be avoided.

In the preceding analysis, we generate mock observations for four emerging probes based on specific experimental setups (each probe being associated with a particular telescope). However, each probe actually has multiple planned observational facilities, and the observational constraints for a single probe can be enhanced through multi-experiment joint observations. Improving the measurement capabilities of individual probes is an important and worthwhile direction for further breaking parameter degeneracies. For FRB observations, future facilities such as FASTA [64], DSA-2000 [65], CHORD [66] and BURSTT [67] will all be powerful tools for FRB detection and localization. For GW observations, ground-based detectors like CE [68], the space-based observatory LISA [69–71], Taiji [72], TianQin [73–76], DECIGO [77] and pulsar timing arrays experiments (such as SKA) will play crucial roles. Furthermore, the multi-band joint GW observations could improve the constraints [78]. For a brief review of GW standard siren cosmology, we refer the reader to Ref. [79]. For SGL observations, CSST is

also expected to discover a large number of SGL systems [80]. For 21 cm IM observations, facilities like SKA [81–83], CHIME [84], and FASTA [85] will also be valuable, and the joint survey strategies worth pursuing [85, 86]. Note that the 21 cm IM method essentially measures the BAO signal, and some galaxy surveys (such as DESI [87, 88] and Euclid [89]) could also be combined with FRB observations, which is worth considering. Additionally, combining SN observations with FRB observations could be explored, provided that the absolute magnitude of type Ia supernova are well understood. Since the physical mechanisms for breaking parameter degeneracies remain constant, our proposed method in this paper can be applied in the future to simultaneously achieve precise measurements of  $H_0$  and  $\Omega_b$ .

#### IV. CONCLUSIONS

This work demonstrates that FRBs, when combined with other emerging cosmological probes, can serve as a powerful tool for simultaneously constraining the Hubble constant  $H_0$  and the cosmic baryon density  $\Omega_b$ —two key parameters whose precise measurement is crucial for addressing the Hubble tension and resolving the missing baryon problem. By breaking the intrinsic degeneracy in FRB dispersion measures through synergy with GW standard sirens, SGL time delays, and 21 cm IM surveys, we achieve high-precision constraints on  $H_0$  and  $\Omega_b$  across a range of cosmological models.

Among the multi-probe strategies considered, the combinations FRB+GW, FRB+SGL, and FRB+21 cm IM all enable simultaneous inference of  $H_0$  and  $\Omega_b$  with remarkable precision that degrades gracefully with increasing model complexity. In the minimal  $\Lambda$ CDM scenario, each synergy achieves sub-percent constraints on both parameters, specifically, better than (1%, 1%) precision for  $(H_0, \Omega_b)$ . As dark energy dynamics are in-

troduced, the uncertainties modestly increase: to better than (1.5%, 2%) precision in the  $w$ CDM model, and to approximately (2%, 3.5%) precision in the more flexible CPL parametrization. Notably, even in the cosmographic, model-independent framework that makes no assumptions about the dark energy sector, FRB+GW and FRB+SGL maintain high reliability, delivering unbiased constraints on  $H_0$  and  $\Omega_b$  at the (1%, 2%) level. This robustness across theoretical paradigms underscores their potential as self-consistent tools for jointly probing cosmic expansion and baryonic matter content.

Our analysis is based on specific experimental designs and observational programs. In practice, a single probe can be implemented through multiple experiments, and its measurement capability can be strengthened by combining data from different experiments or observational bands. Such combinations within a single probe, together with the cross-probe synergies studied here, will reduce statistical uncertainties and help control systematic errors. Because the relationship between the  $H_0$  and  $\Omega_b$  in FRB dispersion measures comes from fundamental physical scaling laws, our method does not depend strongly on specific instrument details and will remain applicable as data quality improves. It therefore offers a reliable way to simultaneously constrain  $H_0$  and  $\Omega_b$ , potentially offering a pathway to resolve both the Hubble tension and the missing baryon problem.

#### ACKNOWLEDGMENTS

This work was supported by the National Natural Science Foundation of China (Grants Nos. 12533001, 12575049, and 12473001), the National SKA Program of China (Grants Nos. 2022SKA0110200 and 2022SKA0110203), the China Manned Space Program (Grant No. CMS-CSST-2025-A02), and the National 111 Project (Grant No. B16009).

---

[1] L. Verde, T. Treu, and A. G. Riess, “Tensions between the Early and the Late Universe,” *Nature Astron.* **3**, 891 (2019), [arXiv:1907.10625 \[astro-ph.CO\]](#).

[2] Adam G. Riess *et al.*, “A Comprehensive Measurement of the Local Value of the Hubble Constant with  $1 \text{ km s}^{-1} \text{ Mpc}^{-1}$  Uncertainty from the Hubble Space Telescope and the SH0ES Team,” *Astrophys. J. Lett.* **934**, L7 (2022), [arXiv:2112.04510 \[astro-ph.CO\]](#).

[3] M. Fukugita, C. J. Hogan, and P. J. E. Peebles, “The Cosmic baryon budget,” *Astrophys. J.* **503**, 518 (1998), [arXiv:astro-ph/9712020](#).

[4] Renyue Cen and Jeremiah P. Ostriker, “Where are the baryons?” *Astrophys. J.* **514**, 1–6 (1999), [arXiv:astro-ph/9806281](#).

[5] J. Michael Shull, Britton D. Smith, and Charles W. Danforth, “The Baryon Census in a Multiphase Intergalactic Medium: 30% of the Baryons May Still Be Missing,” *Astrophys. J.* **759**, 23 (2012), [arXiv:1112.2706 \[astro-ph.CO\]](#).

[6] N. Aghanim *et al.* (Planck), “Planck 2018 results. VI. Cosmological parameters,” *Astron. Astrophys.* **641**, A6 (2020), [Erratum: *Astron. Astrophys.* 652, C4 (2021)], [arXiv:1807.06209 \[astro-ph.CO\]](#).

[7] Steffen Hagstotz, Robert Reischke, and Robert Lilow, “A new measurement of the Hubble constant using fast radio bursts,” *Mon. Not. Roy. Astron. Soc.* **511**, 662–667 (2022), [arXiv:2104.04538 \[astro-ph.CO\]](#).

[8] Qin Wu, Guo-Qiang Zhang, and Fa-Yin Wang, “An 8 per cent determination of the Hubble constant from localized fast radio bursts,” *Mon. Not. Roy. Astron. Soc.* **515**, L1–L5 (2022), [Erratum: *Mon. Not. Roy. Astron. Soc.* 531, L8 (2024)], [arXiv:2108.00581 \[astro-ph.CO\]](#).

[9] Yang Liu, Hongwei Yu, and Puxun Wu, “Cosmological-model-independent Determination of Hubble Constant from Fast Radio Bursts and Hubble Parameter Measurements,” *Astrophys. J. Lett.* **946**, L49 (2023),

arXiv:2210.05202 [astro-ph.CO].

[10] C. W. James *et al.*, “A measurement of Hubble’s Constant using Fast Radio Bursts,” *Mon. Not. Roy. Astron. Soc.* **516**, 4862–4881 (2022), arXiv:2208.00819 [astro-ph.CO].

[11] Jay Baptista, J. Xavier Prochaska, Alexandra G. Manings, C. W. James, R. M. Shannon, Stuart D. Ryder, A. T. Deller, Danica R. Scott, Marcin Glowacki, and Nicolas Tejos, “Measuring the Variance of the Macquart Relation in Redshift–Extragalactic Dispersion Measure Modeling,” *Astrophys. J.* **965**, 57 (2024), arXiv:2305.07022 [astro-ph.CO].

[12] Jéferson A. S. Fortunato, Wiliam S. Hipólito-Ricaldi, and Marcelo V. dos Santos, “Cosmography from well-localized fast radio bursts,” *Mon. Not. Roy. Astron. Soc.* **526**, 1773–1782 (2023), arXiv:2307.04711 [astro-ph.CO].

[13] Jiaze Gao, Zhihuan Zhou, Minghui Du, Rui Zou, Jianping Hu, and Lixin Xu, “A Measurement of Hubble Constant Using Cosmographic Approach from Fast Radio Bursts and SNe Ia,” (2023), arXiv:2307.08285 [astro-ph.CO].

[14] Jun-Jie Wei and Fulvio Melia, “Investigating Cosmological Models and the Hubble Tension Using Localized Fast Radio Bursts,” *Astrophys. J.* **955**, 101 (2023), arXiv:2308.05918 [astro-ph.CO].

[15] Ze-Wei Zhao, Ji-Guo Zhang, Yichao Li, Jing-Fei Zhang, and Xin Zhang, “FRB dark sirens: Measuring the Hubble constant with unlocalized fast radio bursts,” (2022), arXiv:2212.13433 [astro-ph.CO].

[16] Ji-Guo Zhang, Ze-Wei Zhao, Yichao Li, Jing-Fei Zhang, Di Li, and Xin Zhang, “Cosmology with fast radio bursts in the era of SKA,” *Sci. China Phys. Mech. Astron.* **66**, 120412 (2023), arXiv:2307.01605 [astro-ph.CO].

[17] Yi-Ying Wang, Shi-Jie Gao, and Yi-Zhong Fan, “Probing Cosmology with 92 Localized Fast Radio Bursts and DESI BAO,” *Astrophys. J.* **981**, 9 (2025), arXiv:2501.09260 [astro-ph.CO].

[18] Ji-Guo Zhang, Yi-Fan Jiang, Ze-Wei Zhao, Jing-Zhao Qi, Jing-Fei Zhang, and Xin Zhang, “Combining strongly lensed and unlensed fast radio bursts: To be a more precise late-universe probe,” *Sci. China Phys. Mech. Astron.* **68**, 280406 (2025), arXiv:2411.03126 [astro-ph.CO].

[19] Tsung-Ching Yang, Tetsuya Hashimoto, Tzu-Yin Hsu, Tomotsugu Goto, Chih-Teng Ling, Simon C. C. Ho, Amos Y. A. Chen, and Ece Kilerci, “Constraining the Hubble constant with scattering in host galaxies of fast radio bursts,” *Astron. Astrophys.* **693**, A85 (2025), arXiv:2411.02249 [astro-ph.CO].

[20] Surajit Kalita, Shruti Bhatporia, and Amanda Weltman, “Fast Radio Bursts as probes of the late-time universe: A new insight on the Hubble tension,” *Phys. Dark Univ.* **48**, 101926 (2025), arXiv:2410.01974 [astro-ph.CO].

[21] Lázaro L. Sales, Klecio E. L. de Farias, Amilcar R. Queiroz, João R. L. Santos, Rafael A. Batista, Ana R. M. Oliveira, Lucas F. Santana, Carlos A. Wuensche, Thyrso Villela, and Jordany Vieira, “Model-independent observational constraints with fast radio bursts,” (2025), arXiv:2507.06975 [astro-ph.CO].

[22] D. H. Gao, Q. Wu, J. P. Hu, S. X. Yi, X. Zhou, F. Y. Wang, and Z. G. Dai, “Measuring the Hubble constant using localized and nonlocalized fast radio bursts,” *Astron. Astrophys.* **698**, A215 (2025), arXiv:2410.03994 [astro-ph.CO].

[23] Zi-Liang Zhang and Bing Zhang, “Cosmological Parameter Estimate from Persistent Radio Sources of Fast Radio Bursts,” *Astrophys. J. Lett.* **984**, L40 (2025), arXiv:2504.13132 [astro-ph.CO].

[24] Matthew McQuinn, “Locating the “missing” baryons with extragalactic dispersion measure estimates,” *Astrophys. J. Lett.* **780**, L33 (2014), arXiv:1309.4451 [astro-ph.CO].

[25] Wei Deng and Bing Zhang, “Cosmological Implications of Fast Radio Burst/Gamma-Ray Burst Associations,” *Astrophys. J. Lett.* **783**, L35 (2014), arXiv:1401.0059 [astro-ph.HE].

[26] J. P. Macquart *et al.*, “A census of baryons in the Universe from localized fast radio bursts,” *Nature* **581**, 391–395 (2020), arXiv:2005.13161 [astro-ph.CO].

[27] K. B. Yang, Q. Wu, and F. Y. Wang, “Finding the Missing Baryons in the Intergalactic Medium with Localized Fast Radio Bursts,” *Astrophys. J. Lett.* **940**, L29 (2022), arXiv:2211.04058 [astro-ph.HE].

[28] Liam Connor *et al.*, “A gas-rich cosmic web revealed by the partitioning of the missing baryons,” *Nature Astron.* **9**, 1226–1239 (2025), arXiv:2409.16952 [astro-ph.CO].

[29] Ji-Guo Zhang, Ji-Yu Song, Ze-Wei Zhao, Wan-Peng Sun, Jing-Fei Zhang, and Xin Zhang, “Cosmic baryon census with fast radio bursts and gravitational waves,” (2025), arXiv:2507.06841 [astro-ph.CO].

[30] Yang Liu, Yuchen Zhang, Hongwei Yu, and Puxun Wu, “Constraining the Baryon Fraction in the Intergalactic Medium with 92 localized Fast Radio Bursts,” (2025), arXiv:2506.03536 [astro-ph.CO].

[31] D. R. Lorimer, M. Bailes, M. A. McLaughlin, D. J. Narkevic, and F. Crawford, “A bright millisecond radio burst of extragalactic origin,” *Science* **318**, 777 (2007), arXiv:0709.4301 [astro-ph].

[32] D. Thornton *et al.*, “A Population of Fast Radio Bursts at Cosmological Distances,” *Science* **341**, 53–56 (2013), arXiv:1307.1628 [astro-ph.HE].

[33] E. Petroff, J. W. T. Hessels, and D. R. Lorimer, “Fast Radio Bursts,” *Astron. Astrophys. Rev.* **27**, 4 (2019), arXiv:1904.07947 [astro-ph.HE].

[34] B. C. Andersen *et al.* (CHIME/FRB), “A bright millisecond-duration radio burst from a Galactic magnetar,” *Nature* **587**, 54–58 (2020), arXiv:2005.10324 [astro-ph.HE].

[35] Christopher D. Bochenek, Vikram Ravi, Konstantin V. Belov, Gregg Hallinan, Jonathon Kocz, Shri R. Kulkarni, and Dan L. McKenna, “A fast radio burst associated with a Galactic magnetar,” *Nature* **587**, 59–62 (2020), arXiv:2005.10828 [astro-ph.HE].

[36] Bernard F. Schutz, “Determining the Hubble Constant from Gravitational Wave Observations,” *Nature* **323**, 310–311 (1986).

[37] Daniel E. Holz and Scott A. Hughes, “Using gravitational-wave standard sirens,” *Astrophys. J.* **629**, 15–22 (2005), arXiv:astro-ph/0504616.

[38] Tommaso Treu and Philip J. Marshall, “Time Delay Cosmography,” *Astron. Astrophys. Rev.* **24**, 11 (2016), arXiv:1605.05333 [astro-ph.CO].

[39] Philip Bull, Pedro G. Ferreira, Prina Patel, and Mario G. Santos, “Late-time cosmology with 21cm intensity mapping experiments,” *Astrophys. J.* **803**, 21 (2015), arXiv:1405.1452 [astro-ph.CO].

[40] Lu Chen, Qing-Guo Huang, and Ke Wang, “Distance Priors from Planck Final Release,” *JCAP* **02**, 028 (2019), arXiv:1808.05724 [astro-ph.CO].

[41] Mandana Amiri *et al.* (CHIME/FRB), “The First CHIME/FRB Fast Radio Burst Catalog,” *Astrophys. J. Supp.* **257**, 59 (2021), arXiv:2106.04352 [astro-ph.HE].

[42] M. Jaroszynski, “FRBs: the Dispersion Measure of Host Galaxies,” *Acta Astron.* **70**, 87–100 (2020), arXiv:2008.04634 [astro-ph.GA].

[43] Piero Madau and Tassos Fragos, “Radiation Backgrounds at Cosmic Dawn: X-Rays from Compact Binaries,” *Astrophys. J.* **840**, 39 (2017), arXiv:1606.07887 [astro-ph.GA].

[44] Da-Chun Qiang, Shu-Ling Li, and Hao Wei, “Fast radio burst distributions consistent with the first CHIME/FRB catalog,” *JCAP* **01**, 040 (2022), arXiv:2111.07476 [astro-ph.HE].

[45] W. Zhao, C. Van Den Broeck, D. Baskaran, and T. G. F. Li, “Determination of Dark Energy by the Einstein Telescope: Comparing with CMB, BAO and SNIa Observations,” *Phys. Rev. D* **83**, 023005 (2011), arXiv:1009.0206 [astro-ph.CO].

[46] Raffaella Schneider, Valeria Ferrari, Sabino Matarrese, and Simon F. Portegies Zwart, “Gravitational waves from cosmological compact binaries,” *Mon. Not. Roy. Astron. Soc.* **324**, 797 (2001), arXiv:astro-ph/0002055.

[47] Curt Cutler and Daniel E. Holz, “Ultra-high precision cosmology from gravitational waves,” *Phys. Rev. D* **80**, 104009 (2009), arXiv:0906.3752 [astro-ph.CO].

[48] Jing-Fei Zhang, Ming Zhang, Shang-Jie Jin, Jing-Zhao Qi, and Xin Zhang, “Cosmological parameter estimation with future gravitational wave standard siren observation from the Einstein Telescope,” *JCAP* **09**, 068 (2019), arXiv:1907.03238 [astro-ph.CO].

[49] Shang-Jie Jin, Dong-Ze He, Yidong Xu, Jing-Fei Zhang, and Xin Zhang, “Forecast for cosmological parameter estimation with gravitational-wave standard siren observation from the Cosmic Explorer,” *JCAP* **03**, 051 (2020), arXiv:2001.05393 [astro-ph.CO].

[50] Peng-Ju Wu, Yue Shao, Shang-Jie Jin, and Xin Zhang, “A path to precision cosmology: synergy between four promising late-universe cosmological probes,” *JCAP* **06**, 052 (2023), arXiv:2202.09726 [astro-ph.CO].

[51] Shang-Jie Jin, Ye-Zhu Zhang, Ji-Yu Song, Jing-Fei Zhang, and Xin Zhang, “Taiji-TianQin-LISA network: Precisely measuring the Hubble constant using both bright and dark sirens,” *Sci. China Phys. Mech. Astron.* **67**, 220412 (2024), arXiv:2305.19714 [astro-ph.CO].

[52] Ling-Feng Wang, Shang-Jie Jin, Jing-Fei Zhang, and Xin Zhang, “Forecast for cosmological parameter estimation with gravitational-wave standard sirens from the LISA-Taiji network,” *Sci. China Phys. Mech. Astron.* **65**, 210411 (2022), arXiv:2101.11882 [gr-qc].

[53] Si-Ren Xiao, Ji-Yu Song, Yue Shao, Ling-Feng Wang, Jing-Fei Zhang, and Xin Zhang, “Efficient pulsar distance measurement with multiple nanohertz gravitational-wave sources,” (2025), arXiv:2512.10729 [gr-qc].

[54] Ya-Nan Du, Ji-Yu Song, Yichao Li, Shang-Jie Jin, Ling-Feng Wang, Jing-Fei Zhang, and Xin Zhang, “Synergy between CSST and third-generation gravitational-wave detectors: Inferring cosmological parameters using cross-correlation of dark sirens and galaxies,” (2025), arXiv:2510.21521 [astro-ph.CO].

[55] Christopher M. Hirata, Daniel E. Holz, and Curt Cutler, “Reducing the weak lensing noise for the gravitational wave Hubble diagram using the non-Gaussianity of the magnification distribution,” *Phys. Rev. D* **81**, 124046 (2010), arXiv:1004.3988 [astro-ph.CO].

[56] Christopher Gordon, Kate Land, and Anze Slosar, “Cosmological Constraints from Type Ia Supernovae Peculiar Velocity Measurements,” *Phys. Rev. Lett.* **99**, 081301 (2007), arXiv:0705.1718 [astro-ph].

[57] Rong-Gen Cai and Tao Yang, “Estimating cosmological parameters by the simulated data of gravitational waves from the Einstein Telescope,” *Phys. Rev. D* **95**, 044024 (2017), arXiv:1608.08008 [astro-ph.CO].

[58] Thomas E Collett, “The population of galaxy-galaxy strong lenses in forthcoming optical imaging surveys,” *Astrophys. J.* **811**, 20 (2015), arXiv:1507.02657 [astro-ph.CO].

[59] Jingzhao Qi, Shuo Cao, Marek Biesiada, Xuheng Ding, Zong-Hong Zhu, and Xiaogang Zheng, “Strongly gravitationally lensed type Ia supernovae: Direct test of the Friedman-Lemaître-Robertson-Walker metric,” *Phys. Rev. D* **100**, 023530 (2019), arXiv:1802.05532 [astro-ph.CO].

[60] L. B. Newburgh *et al.*, “HIRAX: A Probe of Dark Energy and Radio Transients,” *Proc. SPIE Int. Soc. Opt. Eng.* **9906**, 99065X (2016), arXiv:1607.02059 [astro-ph.IM].

[61] Antony Lewis, Anthony Challinor, and Anthony Lasenby, “Efficient computation of CMB anisotropies in closed FRW models,” *Astrophys. J.* **538**, 473–476 (2000), arXiv:astro-ph/9911177.

[62] Michel Chevallier and David Polarski, “Accelerating universes with scaling dark matter,” *Int. J. Mod. Phys. D* **10**, 213–224 (2001), arXiv:gr-qc/0009008.

[63] Eric V. Linder, “Exploring the expansion history of the universe,” *Phys. Rev. Lett.* **90**, 091301 (2003), arXiv:astro-ph/0208512.

[64] Mengyao Xue, Weiwei Zhu, Xiangping Wu, Renxin Xu, and Hongguang Wang, “Pulsar Discovery Prospect of FASTA,” *Res. Astron. Astrophys.* **23**, 095005 (2023), arXiv:2307.03422 [astro-ph.HE].

[65] G. Hallinan *et al.*, “The DSA-2000 – A Radio Survey Camera,” (2019), arXiv:1907.07648 [astro-ph.IM].

[66] K. Vanderlinde *et al.*, “LRP 2020 Whitepaper: The Canadian Hydrogen Observatory and Radio-transient Detector (CHORD),” (2019), 10.5281/zenodo.3765414, arXiv:1911.01777 [astro-ph.IM].

[67] Hsiao-Hsien Lin *et al.*, “BURSTT: Bustling Universe Radio Survey Telescope in Taiwan,” *Publ. Astron. Soc. Pac.* **134**, 094106 (2022), arXiv:2206.08983 [astro-ph.IM].

[68] David Reitze *et al.*, “Cosmic Explorer: The U.S. Contribution to Gravitational-Wave Astronomy beyond LIGO,” *Bull. Am. Astron. Soc.* **51**, 035 (2019), arXiv:1907.04833 [astro-ph.IM].

[69] Pau Amaro-Seoane *et al.* (LISA), “Laser Interferometer Space Antenna,” (2017), arXiv:1702.00786 [astro-ph.IM].

[70] Travis Robson, Neil J. Cornish, and Chang Liu, “The construction and use of LISA sensitivity curves,” *Class. Quant. Grav.* **36**, 105011 (2019), arXiv:1803.01944 [astro-ph.HE].

[71] Pierre Auclair *et al.* (LISA Cosmology Working Group), “Cosmology with the Laser Interferometer Space Antenna,” *Living Rev. Rel.* **26**, 5 (2023), arXiv:2204.05434 [astro-ph.CO].

[72] Wen-Hong Ruan, Zong-Kuan Guo, Rong-Gen Cai, and Yuan-Zhong Zhang, “Taiji program: Gravitational-wave sources,” *Int. J. Mod. Phys. A* **35**, 2050075 (2020),

arXiv:1807.09495 [gr-qc].

[73] Jun Luo *et al.* (TianQin), “TianQin: a space-borne gravitational wave detector,” *Class. Quant. Grav.* **33**, 035010 (2016), arXiv:1512.02076 [astro-ph.IM].

[74] Shuai Liu, Yi-Ming Hu, Jian-dong Zhang, and Jianwei Mei, “Science with the TianQin observatory: Preliminary results on stellar-mass binary black holes,” *Phys. Rev. D* **101**, 103027 (2020), arXiv:2004.14242 [astro-ph.HE].

[75] Hai-Tian Wang *et al.*, “Science with the TianQin observatory: Preliminary results on massive black hole binaries,” *Phys. Rev. D* **100**, 043003 (2019), arXiv:1902.04423 [astro-ph.HE].

[76] Jianwei Mei *et al.* (TianQin), “The TianQin project: current progress on science and technology,” *PTEP* **2021**, 05A107 (2021), arXiv:2008.10332 [gr-qc].

[77] Seiji Kawamura *et al.*, “The Japanese space gravitational wave antenna: DECIGO,” *Class. Quant. Grav.* **28**, 094011 (2011).

[78] Shang-Jie Jin, Shuang-Shuang Xing, Yue Shao, Jing-Fei Zhang, and Xin Zhang, “Joint constraints on cosmological parameters using future multi-band gravitational wave standard siren observations\*,” *Chin. Phys. C* **47**, 065104 (2023), arXiv:2301.06722 [astro-ph.CO].

[79] Shang-Jie Jin, Ji-Yu Song, Tian-Yang Sun, Si-Ren Xiao, He Wang, Ling-Feng Wang, Jing-Fei Zhang, and Xin Zhang, “Gravitational wave standard sirens: A brief review of cosmological parameter estimation,” (2025), arXiv:2507.12965 [astro-ph.CO].

[80] Xiaoyue Cao *et al.*, “CSST strong lensing preparation: forecasting the galaxy–galaxy strong lensing population for the China space station telescope,” *Mon. Not. Roy. Astron. Soc.* **533**, 1960–1975 (2024), arXiv:2312.06239 [astro-ph.GA].

[81] Mario G. Santos *et al.*, “Cosmology from a SKA HI intensity mapping survey,” *PoS AASKA14*, 019 (2015), arXiv:1501.03989 [astro-ph.CO].

[82] David J. Bacon *et al.* (SKA), “Cosmology with Phase 1 of the Square Kilometre Array: Red Book 2018: Technical specifications and performance forecasts,” *Publ. Astron. Soc. Austral.* **37**, e007 (2020), arXiv:1811.02743 [astro-ph.CO].

[83] Peng-Ju Wu and Xin Zhang, “Prospects for measuring dark energy with 21 cm intensity mapping experiments,” *JCAP* **01**, 060 (2022), arXiv:2108.03552 [astro-ph.CO].

[84] Mandana Amiri *et al.* (CHIME), “An Overview of CHIME, the Canadian Hydrogen Intensity Mapping Experiment,” *Astrophys. J. Supp.* **261**, 29 (2022), arXiv:2201.07869 [astro-ph.IM].

[85] Jun-Da Pan, Peng-Ju Wu, Guo-Hong Du, Yichao Li, and Xin Zhang, “Prospects for cosmological research with the FAST array: 21-cm intensity mapping survey observation strategies,” *JCAP* **01**, 080 (2025), arXiv:2408.00268 [astro-ph.CO].

[86] Peng-Ju Wu, Yichao Li, Jing-Fei Zhang, and Xin Zhang, “Prospects for measuring dark energy with 21 cm intensity mapping experiments: A joint survey strategy,” *Sci. China Phys. Mech. Astron.* **66**, 270413 (2023), arXiv:2212.07681 [astro-ph.CO].

[87] A. G. Adame *et al.* (DESI), “DESI 2024 VI: cosmological constraints from the measurements of baryon acoustic oscillations,” *JCAP* **02**, 021 (2025), arXiv:2404.03002 [astro-ph.CO].

[88] M. Abdul Karim *et al.* (DESI), “DESI DR2 results. II. Measurements of baryon acoustic oscillations and cosmological constraints,” *Phys. Rev. D* **112**, 083515 (2025), arXiv:2503.14738 [astro-ph.CO].

[89] Luca Amendola *et al.*, “Cosmology and fundamental physics with the Euclid satellite,” *Living Rev. Rel.* **21**, 2 (2018), arXiv:1606.00180 [astro-ph.CO].